

High performance organic sensitizers based on 11,12-bis(hexyloxy) dibenzo[*a,c*]phenazine for dye-sensitized solar cellsJie Shi,<sup>a</sup> Junnian Chen,<sup>a</sup> Zhaofei Chai,<sup>a</sup> Heng Wang,<sup>b</sup> Runli Tang,<sup>a</sup> Ke Fan,<sup>a</sup> Mei Wu,<sup>a</sup> Hongwei Han,<sup>b</sup> Jingui Qin,<sup>a</sup> Tianyou Peng,<sup>a</sup> Qianqian Li<sup>\*a</sup> and Zhen Li<sup>\*a</sup>

Received 14th June 2012, Accepted 24th July 2012

DOI: 10.1039/c2jm33833e

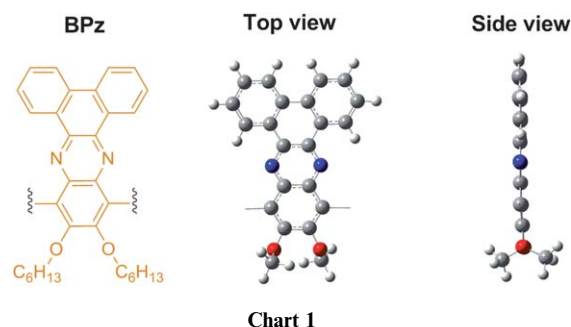
Three new metal-free organic sensitizers containing 11,12-bis(hexyloxy) dibenzo[*a,c*]phenazine (BPz) units were synthesized and used for dye-sensitized solar cells (DSSCs). The broad absorption spectra indicate that the light harvesting abilities were enhanced by the introduction of the BPz unit in the  $\pi$ -conjugated space, which can also cause an anti-aggregation effect and the suppression of charge recombination. Among these sensitizers, **LI-39** showed the best photovoltaic performance: a short-circuit photocurrent density ( $J_{sc}$ ) of 14.40 mA cm<sup>-2</sup>, an open-circuit photovoltage ( $V_{oc}$ ) of 0.74 V, and a fill factor (ff) of 0.67, corresponding to an overall conversion efficiency of 7.18% under standard global AM 1.5 solar light conditions. The result shows that the organic sensitizers based on this bulky fused aromatic rings as well as the auxiliary acceptor are the promising candidates for improvement of the performance of DSSCs.

## Introduction

Dye-sensitized solar cells (DSSCs), which have been investigated as promising candidates for renewable-energy systems, have attracted great attention in both academic and industrial communities due to their high achievable efficiencies at low cost.<sup>1</sup> In addition to the metal complexes,<sup>2</sup> the metal-free organic sensitizers have also been desirable due to their wide variety of structures, facile modification, and high molar absorption coefficient.<sup>3</sup> Importantly, there is still much room for chemists to improve their cell performance by modifying the structure of the metal-free organic sensitizers. Actually, the  $\pi$ -conjugated spacer, which links the donor (D) and acceptor (A) moieties in the general D- $\pi$ -A structure of metal-free organic sensitizers, plays an important role in intramolecular charge transfer (ICT) efficiency, partially determining the DSSC performances of the corresponding cells.<sup>4</sup> Thus, many efforts have been made to modify the intrinsic electronic characteristics of the  $\pi$ -conjugated spacer.<sup>5</sup> To tune the HOMO and LUMO levels, and broaden the responsive wavelength, an auxiliary acceptor, generally the electron-deficient segment, was introduced to the  $\pi$ -conjugated spacer, to construct a so called "D-A- $\pi$ -A" structure. Applying this idea, Tian and co-workers have reported some sensitizers with good DSSC performance.<sup>6</sup> As it is well known, how to

prevent the intermolecular  $\pi$ - $\pi$  stacking among sensitizers and keep I<sub>3</sub><sup>-</sup> ions away from the TiO<sub>2</sub> electrode surface in the DSSCs is another important requirement for the design of sensitizers, besides the above mentioned electronic properties. Thus, it might be an ideal mode to find a construction block, which could fulfil all the above requirements, to build new sensitizers.

11,12-Bis(hexyloxy) dibenzo[*a,c*]phenazine (BPz), a derivative of quinoxaline, in which the combination of the bis(hexyloxy)-linked quinoxaline and phenanthrene rings resulted in the large extended  $\pi$ -conjugation system on the orthogonal directions with planar configuration, to favor the light harvesting over the solar irradiation (Chart 1). Moreover, the extension of the conjugation system in the orthogonal directions can also act as the isolation group to prevent the intermolecular  $\pi$ - $\pi$  aggregation, and reduce the degree of charge trapping at the electron deficient moiety.<sup>7</sup> With the incorporation of the electron-deficient properties of the quinoxaline unit, this bulky fused aromatic rings with electron-withdrawing character could lead to



<sup>a</sup>Department of Chemistry, Hubei Key Lab on Organic and Polymeric Opto-Electronic Materials, Wuhan University, Wuhan 430072, China. E-mail: qianqian-alinda@163.com; lizhen@whu.edu.cn; lichemlab@163.com; Fax: +86-27-68755363; Tel: +86-27-62254108

<sup>b</sup>Michael Grätzel Center for Mesoscopic Solar Cells, Wuhan National Laboratory for Optoelectronics, Huazhong University of Science and Technology, Wuhan, 430072, China

the broader light absorption as well as the red-shifted absorption spectra. Additionally, the hexyloxy chains, linked to the quinoxaline moiety in the vertical direction, can not only form a blocking layer to keep  $I_3^-$  ions away from the  $TiO_2$  electrode surface, but also increase the solubility of the whole molecule.<sup>8</sup> Thus, this aromatic block might be a good construction one. However, interestingly, there are no reports concerning its utilization in the design of DSSC sensitizers.

In our previous studies, the BPz unit was applied in alternating copolymers with different connecting points as the acceptor. Unexpectedly, the different connecting points led to the completely different photovoltaic performance of the copolymers in the devices of polymer solar cells. These results were very interesting, exhibited the unique properties of this large conjugated system, and hinted that the BPz unit was a good building block to enhance the electron-optical properties of the resulting materials.<sup>9</sup>

Considering all the above points, the BPz unit was incorporated into the conjugated bridge as an auxiliary acceptor to form new sensitizers with the D- $\pi$ -A'- $\pi$ -A configuration, 3-hexylthiophene was chosen as an additional  $\pi$  spacer to link the donor and the auxiliary acceptor (Chart 2). With the aim to optimize the performance of these organic sensitizers, and seek the suitable donor group to match the electron properties of the  $\pi$ -conjugated system, the modulation of the donor units was made to alter the molecular energy levels and the absorption edge. As a result, these sensitizers show evident bathochromic shifts in absorption, and thus effectively improve the light-harvesting range. The best photovoltaic performance of these sensitizers exhibited an overall conversion efficiency of 7.18% under standard global AM 1.5 solar light condition. Herein, we report their syntheses, structural characterization, electrochemical properties, theoretical calculations, and photovoltaic performance.

## Experimental

### Materials

Tetrahydrofuran (THF) and toluene were dried over and distilled from K-Na alloy under an atmosphere of dry nitrogen. *N,N*-Dimethylformamide (DMF) was dried over and distilled from  $CaH_2$  under an atmosphere of dry nitrogen. 1,2-Dichloroethane was dried over and distilled from phosphorus pentoxide. Phosphorus oxychloride was freshly distilled before use. All reagents were purchased from Alfa Aesar or Aldrich and used as received. 3,6-Dibromo-4,5-bis(hexyloxy)benzene-1,2-diamine (compound 5) was prepared following the procedure reported in the literature.<sup>10</sup>

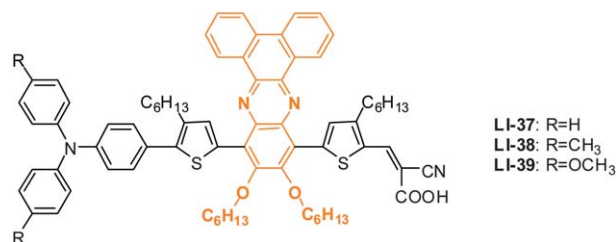


Chart 2

### Instrumentation

$^1H$  and  $^{13}C$  NMR spectroscopy study was conducted with a Varian Mercury 300 spectrometer using tetramethylsilane (TMS;  $\delta = 0$  ppm) as the internal standard. UV-visible spectra were obtained using a Shimadzu UV-2550 spectrometer. Cyclic voltammograms were carried out on a CHI 660 voltammetric analyzer at room temperature in nitrogen-purged anhydrous dichloromethane with tetrabutylammonium hexafluorophosphate (TBAPF<sub>6</sub>) as the supporting electrolyte at a scanning rate of  $100\text{ mV s}^{-1}$ . A platinum disk and a Ag/AgCl electrode were used as the working electrode and quasi-reference electrode, respectively. The ferrocene/ferrocenium redox couple was used for potential calibration. Elemental analyses were performed by a 73 CARLOERBA-1106 micro-elemental analyzer. EI-MS spectra were recorded with a Finnigan PRACE mass spectrometer. Matrix-assisted laser desorption ionization time-of-flight mass spectra were measured on a Voyager-DE-STR MALDI-TOF mass spectrometer (MALDI-TOF MS; ABI, American) equipped with a 337 nm nitrogen laser and a 1.2 m linear flight path in positive ion mode.

### Synthesis

**10,13-Dibromo-11,12-bis(hexyloxy)dibenzo[*a,c*]phenazine (2).** 9,10-Phenanthraquinone (1.50 g, 7.22 mmol), toluene (80 mL) and 3,6-dibromo-4,5-bis(hexyloxy)benzene-1,2-diamine (3.36 g, 7.22 mmol) were placed in a round-bottomed flask fixed with a condenser. The mixture was heated under reflux for 6 h and then allowed to cool to room temperature. The solvent was removed under vacuum. The product was purified by column chromatography to give the product (3.77 g, 82%) as a yellow solid.  $^1H$  NMR ( $CDCl_3$ , 300 MHz)  $\delta$  (ppm): 9.45 (d,  $J = 8.1$  Hz, 2H, ArH), 8.56 (d,  $J = 7.2$  Hz, 2H, ArH), 7.84–7.74 (m, 4H, ArH), 4.29–4.25 (m, 4H,  $-CH_2-$ ), 1.98–1.86 (m, 4H,  $-CH_2-$ ), 1.41 (br, 12H,  $-CH_2-$ ), 0.96–0.93 (m, 6H,  $-CH_3$ ).

**11,12-Bis(hexyloxy)-10,13-bis(4-hexylthiophen-2-yl)dibenzo[*a,c*]phenazine (3).** To a solution of 2 (3.19 g, 5.0 mmol) and tributyl(4-hexylthiophen-2-yl)stannane (4.57 g, 10.0 mmol) in toluene (30 mL) was added  $Pd(PPh_3)_4$  (24 mg, 0.02 mmol) under an atmosphere of dry nitrogen. After refluxing for 12 h, the mixture was cooled to room temperature and then poured into water, the organic layer was extracted by  $CH_2Cl_2$  and dried over anhydrous  $Na_2SO_4$ . The crude product was purified through a silica gel chromatography column to give the product (3.46 g, 85%) as an orange red oil.  $^1H$  NMR ( $CDCl_3$ , 300 MHz)  $\delta$  (ppm): 9.38 (d,  $J = 6.0$  Hz, 2H, ArH), 8.56 (d,  $J = 4.8$  Hz, 2H, ArH), 7.95 (s, 2H, ArH), 7.76–7.72 (m, 4H, ArH), 7.25 (s, 2H, ArH), 4.08 (br, 4H,  $-CH_2-$ ), 2.78 (br, 4H,  $-CH_2-$ ), 1.82 (br, 8H,  $-CH_2-$ ), 1.45–1.25 (m, 24H,  $-CH_2-$ ), 0.92 (br, 12H,  $-CH_3$ ).

**5-(11,12-Bis(hexyloxy)-13-(4-hexylthiophen-2-yl)dibenzo[*a,c*]phenazin-10-yl)-3-hexylthiophene-2-carbaldehyde (4).** DMF (1.07 g, 14.76 mmol) was added to freshly distilled  $POCl_3$  (1.13 g, 7.38 mmol) under an atmosphere of dry nitrogen at  $0^\circ C$ , and the resultant solution was stirred until its complete conversion into a glassy solid. After the addition of compound 3 (3.0 g, 3.69 mmol) in 1,2-dichloroethane (20 mL) dropwise, the mixture was stirred at room temperature overnight, then poured into an aqueous

solution of sodium acetate (1 M, 200 mL), and stirred for another 2 h. The mixture was extracted with chloroform several times, the organic fractions were combined and dried over anhydrous  $\text{Na}_2\text{SO}_4$ . After removing the solvent under vacuum, the crude product was purified through a silica gel chromatography column to give the product (2.04 g, 65%) as a red oil.  $^1\text{H}$  NMR ( $\text{CDCl}_3$ , 300 MHz)  $\delta$  (ppm): 10.23 (s, 1H, -CHO), 9.38 (d,  $J = 6.3$  Hz, 1H, ArH), 9.29 (d,  $J = 7.2$  Hz, 1H, ArH), 8.57 (d,  $J = 6.9$  Hz, 2H, ArH), 7.98 (d,  $J = 4.8$  Hz, 2H, ArH), 7.79–7.74 (m, 4H, ArH), 7.25 (s, 1H, ArH), 4.12 (br, 4H,  $-\text{CH}_2-$ ), 2.74 (br, 4H,  $-\text{CH}_2-$ ), 1.85 (br, 8H,  $-\text{CH}_2-$ ), 1.48–1.37 (m, 24H,  $-\text{CH}_2-$ ), 0.92 (br, 12H,  $-\text{CH}_3$ ).

**5-(13-(5-Bromo-4-hexylthiophen-2-yl)-11,12-bis(hexyloxy)dibenzo[*a,c*]phenazin-10-yl)-3-hexylthiophene-2-carbaldehyde (5).** To a solution of compound **4** (1.99 g, 2.4 mmol) in  $\text{CHCl}_3$  (20 mL) was added *N*-bromosuccinimide (0.45 g, 2.5 mmol). This mixture was stirred for 10 h in the absence of light at room temperature and then the solvent was removed under vacuum. The crude product was purified through a silica gel chromatography column to give the product (1.75 g, 79%) as a red solid.  $^1\text{H}$  NMR ( $\text{CDCl}_3$ , 300 MHz)  $\delta$  (ppm): 10.20 (s, 1H, -CHO), 9.31 (d,  $J = 6.1$  Hz, 1H, ArH), 9.25 (d,  $J = 6.5$  Hz, 1H, ArH), 8.54 (d,  $J = 6.4$  Hz, 2H, ArH), 7.90 (d,  $J = 5.3$  Hz, 2H, ArH), 7.71–7.79 (m, 4H, ArH), 4.18 (br, 4H,  $-\text{CH}_2-$ ), 2.71 (br, 4H,  $-\text{CH}_2-$ ), 1.88 (br, 8H,  $-\text{CH}_2-$ ), 1.42–1.36 (m, 24H,  $-\text{CH}_2-$ ), 0.91 (br, 12H,  $-\text{CH}_3$ ).

**General synthesis of 6.** A mixture of **5** (0.60 g, 0.65 mmol), 4-(diphenylamino) phenylboronic acid, 4-(diptolylamino) phenylboronic acid or 4-(bis(4-methoxyphenyl)amino) phenylboronic acid (1.0 mmol), sodium carbonate (0.69 g, 6.5 mmol), THF (monomer concentration about 0.025 M)/water (2 : 1 in volume), and  $\text{Pd}(\text{PPh}_3)_4$  (10 mg) was carefully degassed and charged with nitrogen. The reaction was stirred for 24 h at 80 °C. After cooled to room temperature, the organic layer was separated, dried over anhydrous  $\text{Na}_2\text{SO}_4$ , and evaporated to dryness. The crude product was purified by column chromatography over silica gel to give product.

**5-(13-(5-(4-(Diphenylamino)phenyl)-4-hexylthiophen-2-yl)-11,12-bis(hexyloxy)dibenzo[*a,c*]phenazin-10-yl)-3-hexylthiophene-2-carbaldehyde (6a).** Dark red solid. 0.52 g. Yield: 74%.  $^1\text{H}$  NMR ( $\text{CDCl}_3$ , 300 MHz)  $\delta$  (ppm): 10.22 (s, 1H, -CHO), 9.48 (d,  $J = 7.8$  Hz, 1H, ArH), 9.32 (d,  $J = 8.7$  Hz, 1H, ArH), 8.59 (d,  $J = 7.8$  Hz, 2H, ArH), 8.10 (s, 1H, ArH), 7.99 (s, 1H, ArH), 7.79–7.71 (m, 4H, ArH), 7.52 (d,  $J = 8.7$  Hz, 2H, ArH), 7.31 (d,  $J = 7.8$  Hz, 1H, ArH), 7.10–6.94 (m, 9H, ArH), 6.77 (d,  $J = 9.0$  Hz, 2H, ArH), 4.23–4.12 (m, 4H,  $-\text{CH}_2-$ ), 2.85 (br, 4H,  $-\text{CH}_2-$ ), 1.88 (br, 8H,  $-\text{CH}_2-$ ), 1.46–1.34 (m, 24H,  $-\text{CH}_2-$ ), 0.91 (br, 12H,  $-\text{CH}_3$ ).

**5-(13-(5-(4-(Dip-tolylamino)phenyl)-4-hexylthiophen-2-yl)-11,12-bis(hexyloxy)dibenzo[*a,c*]phenazin-10-yl)-3-hexylthiophene-2-carbaldehyde (6b).** Dark red solid. 0.48 g. Yield: 66%.  $^1\text{H}$  NMR ( $\text{CDCl}_3$ , 300 MHz)  $\delta$  (ppm): 10.22 (s, 1H, -CHO), 9.49 (d,  $J = 7.2$  Hz, 1H, ArH), 9.32 (d,  $J = 8.1$  Hz, 1H, ArH), 8.61 (d,  $J = 6.3$  Hz, 2H, ArH), 8.10 (s, 1H, ArH), 7.99 (s, 1H, ArH), 7.78–7.73 (m, 4H, ArH), 7.47 (d,  $J = 7.6$  Hz, 2H, ArH), 7.33 (d,  $J = 7.8$  Hz, 1H, ArH), 7.13–6.91 (m, 7H, ArH), 6.78 (d,  $J = 8.1$  Hz, 2H, ArH), 4.13 (br, 4H,  $-\text{CH}_2-$ ), 2.85 (br, 4H,  $-\text{CH}_2-$ ), 2.34 (br, 6H,  $-\text{CH}_3$ ), 1.86 (br, 8H,  $-\text{CH}_2-$ ), 1.46–1.34 (m, 24H,  $-\text{CH}_2-$ ), 0.91 (br, 12H,  $-\text{CH}_3$ ).

**5-(13-(5-(4-(Bis(4-methoxyphenyl)amino)phenyl)-4-hexylthiophen-2-yl)-11,12-bis(hexyloxy)dibenzo[*a,c*]phenazin-10-yl)-3-hexylthiophene-2-carbaldehyde (6c).** Dark red solid. 0.54 g. Yield: 72%.  $^1\text{H}$  NMR ( $\text{CDCl}_3$ , 300 MHz)  $\delta$  (ppm): 10.21 (s, 1H, -CHO), 9.45 (d,  $J = 7.6$  Hz, 1H, ArH), 9.40 (d,  $J = 7.2$  Hz, 1H, ArH), 8.67 (d,  $J = 6.5$  Hz, 2H, ArH), 8.12 (s, 1H, ArH), 7.99 (s, 1H, ArH), 7.76–7.71 (m, 4H, ArH), 7.46 (d,  $J = 7.8$  Hz, 2H, ArH), 7.34 (d,  $J = 7.8$  Hz, 1H, ArH), 7.12–6.93 (m, 7H, ArH), 6.74 (d,  $J = 8.7$  Hz, 2H, ArH), 4.18 (br, 4H,  $-\text{CH}_2-$ ), 3.82 (br, 6H,  $-\text{CH}_3$ ), 2.85 (br, 4H,  $-\text{CH}_2-$ ), 1.82 (br, 8H,  $-\text{CH}_2-$ ), 1.43–1.34 (m, 24H,  $-\text{CH}_2-$ ), 0.90 (br, 12H,  $-\text{CH}_3$ ).

**General synthesis of sensitizers.** A mixture of **6** (0.2 mmol) and cyanoacetic acid (1.0 mmol) were vacuum-dried, then MeCN (15 mL), THF (5 mL) and piperidine (10  $\mu\text{L}$ ) were added. The solution was refluxed for 8 h. After the solution was cooled, the organic layer was removed under vacuum. The product was purified by column chromatography.

**2-Cyano-3-(5-(13-(5-(4-(diphenylamino)phenyl)-4-hexylthiophen-2-yl)-11,12-bis(hexyloxy)dibenzo[*a,c*]phenazin-10-yl)-3-hexylthiophen-2-yl)acrylic acid (LI-37).** Dark red solid. 0.16 g. Yield: 68%.  $^1\text{H}$  NMR ( $\text{DMSO}-d_6$ , 300 MHz)  $\delta$  (ppm): 9.01 (br, 1H, ArH), 8.91 (br, 1H, ArH), 8.40 (br, 2H, ArH), 8.25 (s, 1H,  $-\text{CH}=\text{C}$ ), 7.89 (s, 1H, ArH), 7.85 (s, 1H, ArH), 7.64–7.54 (m, 4H, ArH), 7.32 (br, 6H, ArH), 7.10 (br, 8H, ArH), 3.83 (br, 4H,  $-\text{CH}_2-$ ), 2.65 (br, 4H,  $-\text{CH}_2-$ ), 1.70 (br, 8H,  $-\text{CH}_2-$ ), 1.35–1.26 (m, 24H,  $-\text{CH}_2-$ ), 0.85 (br, 12H,  $-\text{CH}_3$ ).  $^{13}\text{C}$  NMR ( $\text{DMSO}-d_6$ , 75 MHz)  $\delta$  (ppm): 169.4, 154.6, 152.3, 147.9, 147.3, 145.6, 144.7, 141.5, 140.7, 137.8, 135.1, 134.1, 132.3, 131.1, 130.1, 129.6, 129.2, 127.4, 126.4, 124.9, 123.4, 122.9, 121.9, 116.9, 95.7, 75.1, 74.4, 32.1, 31.7, 30.9, 29.8, 29.6, 26.2, 22.9, 14.4. MALDI-TOF MS calcd for  $\text{C}_{74}\text{H}_{78}\text{N}_4\text{O}_4\text{S}_2$  [ $\text{M}^+$ ]  $m/z$ : 1151.55 [ $\text{M}^+$ ] found.  $\text{C}_{74}\text{H}_{78}\text{N}_4\text{O}_4\text{S}_2$  ( $\text{M}^+$ ): 1151.37. Anal. calcd for  $\text{C}_{74}\text{H}_{78}\text{N}_4\text{O}_4\text{S}_2$ : C, 77.18; H, 6.83; N, 4.87. Found: C, 77.57; H, 7.13; N, 5.05%

**2-Cyano-3-(5-(13-(5-(4-(dip-tolylamino)phenyl)-4-hexylthiophen-2-yl)-11,12-bis(hexyloxy)dibenzo[*a,c*]phenazin-10-yl)-3-hexylthiophen-2-yl)acrylic acid (LI-38).** Dark red solid. 0.14 g. Yield: 59%.  $^1\text{H}$  NMR ( $\text{DMSO}-d_6$ , 300 MHz)  $\delta$  (ppm): 9.30 (d,  $J = 7.5$  Hz, 1H, ArH), 9.21 (d,  $J = 7.2$  Hz, 1H, ArH), 8.57 (d,  $J = 9.0$  Hz, 2H, ArH), 8.42 (s, 1H,  $-\text{CH}=\text{C}$ ), 8.07 (s, 1H, ArH), 8.01 (s, 1H, ArH), 7.74–7.60 (m, 4H, ArH), 7.39 (d,  $J = 8.4$  Hz, 2H, ArH), 7.13 (d,  $J = 8.4$  Hz, 4H, ArH), 7.03 (d,  $J = 7.8$  Hz, 6H, ArH), 4.06 (br, 4H,  $-\text{CH}_2-$ ), 2.87 (br, 4H,  $-\text{CH}_2-$ ), 2.32 (br, 6H,  $-\text{CH}_3$ ), 1.86 (br, 8H,  $-\text{CH}_2-$ ), 1.44–1.34 (m, 24H,  $-\text{CH}_2-$ ), 0.89 (br, 12H,  $-\text{CH}_3$ ).  $^{13}\text{C}$  NMR ( $\text{DMSO}-d_6$ , 75 MHz)  $\delta$  (ppm): 169.8, 154.5, 152.2, 150.7, 147.6, 145.4, 141.6, 140.5, 137.6, 135.2, 133.9, 133.0, 131.8, 130.8, 130.2, 129.9, 128.1, 126.2, 125.2, 123.9, 122.2, 120.8, 116.1, 101.2, 74.9, 74.3, 32.1, 30.9, 29.8, 29.5, 26.2, 22.9, 21.1, 14.4. MALDI-TOF MS calcd for  $\text{C}_{76}\text{H}_{82}\text{N}_4\text{O}_4\text{S}_2$  [ $\text{M}^+$ ]  $m/z$ : 1179.58 [ $\text{M}^+$ ] found.  $\text{C}_{76}\text{H}_{82}\text{N}_4\text{O}_4\text{S}_2$  ( $\text{M}^+$ ): 1179.49. Anal. calcd for  $\text{C}_{76}\text{H}_{82}\text{N}_4\text{O}_4\text{S}_2$ : C, 77.38; H, 7.01; N, 4.75. Found: C, 77.62; H, 7.26; N, 4.67%.

**3-(5-(13-(5-(4-(Bis(4-methoxyphenyl)amino)phenyl)-4-hexylthiophen-2-yl)-11,12-bis(hexyloxy)dibenzo[*a,c*]phenazin-10-yl)-3-hexylthiophen-2-yl)-2-cyanoacrylic acid (LI-39).** Dark red solid. 0.14 g. Yield: 58%.  $^1\text{H}$  NMR ( $\text{DMSO}-d_6$ , 300 MHz)  $\delta$  (ppm):

9.39 (br, 1H, ArH), 9.28 (d,  $J = 8.1$  Hz, 1H, ArH), 8.57 (br, 2H, ArH), 8.45 (s, 1H,  $-\text{CH}=\text{C}$ ), 8.08 (s, 1H, ArH), 8.04 (s, 1H, ArH), 7.78–7.67 (m, 4H, ArH), 7.39 (d,  $J = 8.9$  Hz, 2H, ArH), 7.13 (d,  $J = 8.4$  Hz, 4H, ArH), 6.96–6.89 (m, 6H, ArH), 4.09 (br, 4H,  $-\text{CH}_2-$ ), 3.79 (br, 6H,  $-\text{CH}_3$ ), 2.91 (br, 4H,  $-\text{CH}_2-$ ), 1.85 (br, 8H,  $-\text{CH}_2-$ ), 1.46–1.34 (m, 24H,  $-\text{CH}_2-$ ), 0.90 (br, 12H,  $-\text{CH}_3$ ).  $^{13}\text{C}$  NMR (DMSO- $d_6$ , 75 MHz)  $\delta$  (ppm): 169.0, 156.3, 154.3, 152.2, 148.1, 142.9, 141.9, 141.1, 140.6, 139.0, 137.6, 137.4, 135.0, 133.8, 133.4, 132.8, 132.1, 130.8, 129.9, 137.1, 125.8, 122.1, 120.4, 116.4, 98.5, 74.4, 55.8, 32.1, 31.8, 30.7, 29.8, 29.5, 26.2, 22.9, 14.3. MALDI-TOF MS calcd for  $\text{C}_{76}\text{H}_{82}\text{N}_4\text{O}_6\text{S}_2$  [ $\text{M}^+$ ]  $m/z$ : 1211.57 [ $\text{M}^+$ ] found.  $\text{C}_{76}\text{H}_{82}\text{N}_4\text{O}_6\text{S}_2$  ( $\text{M}^+$ ): 1211.52. Anal. calcd for  $\text{C}_{76}\text{H}_{82}\text{N}_4\text{O}_6\text{S}_2$ : C, 75.34; H, 6.82; N, 4.62. Found: C, 75.03; H, 6.68; N, 4.52%.

### Device fabrication

A layer of *ca.* 2  $\mu\text{m}$   $\text{TiO}_2$  (TPP-3, Heptachroma, China) was coated on the FTO conducting glass by screen printing and then dried for 6 min at 125  $^\circ\text{C}$ . This procedure was repeated 6 times (*ca.* 12  $\mu\text{m}$ ) and finally coated by a layer (*ca.* 4  $\mu\text{m}$ ) of  $\text{TiO}_2$  paste (TPP-200, Heptachroma, China) as the scattering layer. The  $\text{TiO}_2$  electrodes were gradually heated under an air flow at 450  $^\circ\text{C}$  for 30 min. The sintered film was further treated with 0.2 M  $\text{TiCl}_4$  aqueous solution at room temperature for 12 h, then washed with water and ethanol, and annealed at 450  $^\circ\text{C}$  for 30 min. After the film was cooled to 80  $^\circ\text{C}$ , it was immersed in a  $3 \times 10^{-4}$  M sensitizer bath in  $\text{CH}_2\text{Cl}_2$  solution and maintained in the dark for 24 h at room temperature. The electrode was then rinsed with  $\text{CH}_2\text{Cl}_2$  and dried. The size of the  $\text{TiO}_2$  electrodes used was 0.238  $\text{cm}^2$ . To prepare the counter electrode, the Pt catalyst was deposited on cleaned FTO glass by coating with a drop of  $\text{H}_2\text{PtCl}_6$  solution (0.02 M 2-propanol solution) with heat treatment at 400  $^\circ\text{C}$  for 15 min. A hole (0.8 mm diameter) was drilled on the counter electrode using a drill-press. The perforated sheet was cleaned with ultrasound in an ethanol bath for 10 min. For the assembly of DSSCs, the sensitizer-covered  $\text{TiO}_2$  electrode and Pt-counter electrode were assembled into a sandwich type cell and sealed with a hot-melt gasket of 25  $\mu\text{m}$  thickness made of the ionomer Surlyn 1702 (DuPont). The electrolyte (DHS-Z23, Heptachroma, China) was introduced into the cell *via* vacuum backfilling from the hole in the back of the counter electrode. Finally, the hole was sealed using a piece of aluminum foil tape.

### Photovoltaic properties measurements

The DSSC was illuminated by light with energy of a 100  $\text{mW cm}^{-2}$  from 300 W AM 1.5G simulated sunlight ( $2 \times 2$  beam, w/6258 lamp, Newport, USA). The light intensity was determined using a SRC-1000-TC-QZ-N reference monocrystalline silicon cell system (Oriel, USA), which was calibrated by National Renewable Energy Laboratory, A2LA accreditation certificate 2236.01. The current–voltage ( $J$ – $V$ ) curves for the fabricated DSSCs were collected by using CHI618 electrochemical analyzer (CH Instruments). Cell active area was tested with a metal mask of 0.16  $\text{cm}^2$ . The electrochemical impedance spectra (EIS) measurements were carried out with applying bias of the open circuit voltage ( $V_{\text{oc}}$ ) under the conditions and recorded over a frequency range from 0.05 Hz to 105 Hz with an ac amplitude of 10 mV. All of the

measurements mentioned above were taken under ambient conditions. Incident photon-current conversion efficiency (IPCE) was recorded on a DC Power Meter (Model 2931-C, Newport Co.) under irradiation of a 300 W xenon lamp light source with a motorized monochromator (Oriel). The xenon lamp was powered by an Arc Lamp Power Supply (Model 69920, Newport Co.).

## Results and discussion

### Design and synthesis of the sensitizers

The quinoxaline unit was initially utilized to the  $\pi$ -conjugated space of organic sensitizers with the linkage of the *para* position of 2,3-diphenyl rings (Chart 3), as a strong electron-drawing unit. Lately, with the aim of decreasing electron recombination, this unit was further modified by the introduction of alkoxy chains to the phenyl rings (Chart 3).<sup>11</sup> When the 2,3-diphenyl rings were replaced by the phenanthrene unit, and alkoxy chains moved to the quinoxaline ring, BPz unit was formed, which retained the intrinsic electron properties of quinoxaline and the suppression of electron recombination, however, the incorporation of the phenanthrene unit make the conjugated system more planar and larger, as mentioned above, which would be beneficial to the enhancement of the light harvesting abilities.

The sensitizers with the incorporation of BPz unit into the  $\pi$ -conjugated bridge were synthesized according to the synthetic routes in Scheme 1. The important intermediate **2**, BPz unit with the linkage of bromine, was obtained by a cyclization reaction with high yield. After the Stille coupling reaction with tributyl(4-hexylthiophen-2-yl)stannane, the conjugated bridge was formed by the incorporation of BPz unit and hexylthiophene. The introduction of long alkyl chains and alkoxy chains into sensitizers can not only inhibit the dye aggregation but also improve the solubility, which is of great benefit to the synthesis and purification. Compound **4** was obtained by the followed Vilsmeier reaction. For further grafting the donor unit, simple bromination and Suzuki coupling reactions were treated on the reactive hexylthiophene unit, to produce the aldehyde precursor **6**. Finally, the conventional Knoevenagel condensation yielded the final product with cyanoacetic acid in the presence of piperidine. The sensitizers and their precursor compounds are soluble in common organic solvents (*i.e.*, acetone,  $\text{CH}_2\text{Cl}_2$ ,  $\text{CHCl}_3$ , DMF, DMSO and THF). The structure and purity of the three compounds were confirmed by  $^1\text{H}$  NMR,  $^{13}\text{C}$  NMR, MALDI-TOF MS and elemental analysis.

### Optical properties

The absorption spectra of sensitizers in dilute dichloromethane solution are displayed in Fig. 1, and the absorption peaks as well

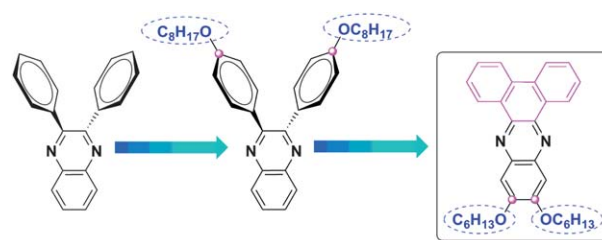
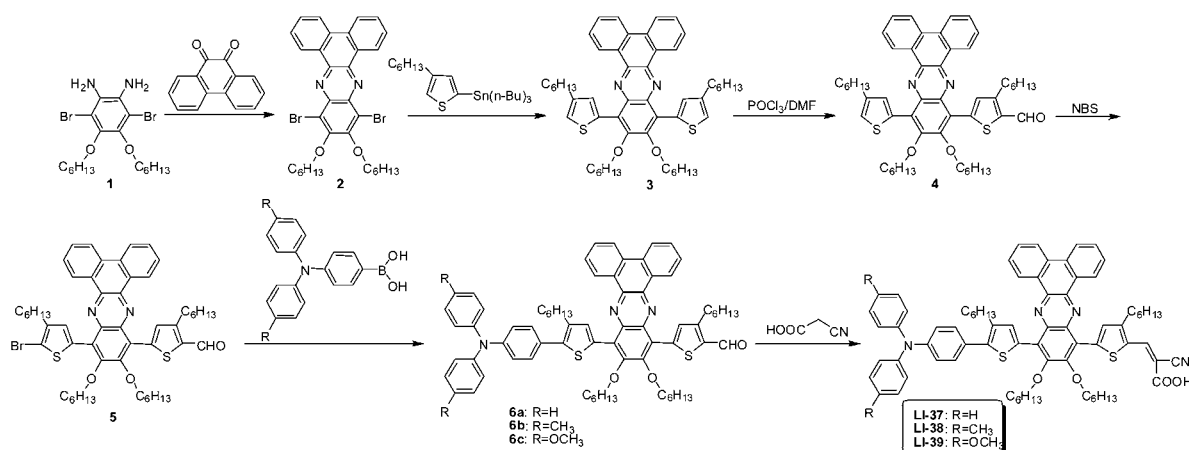
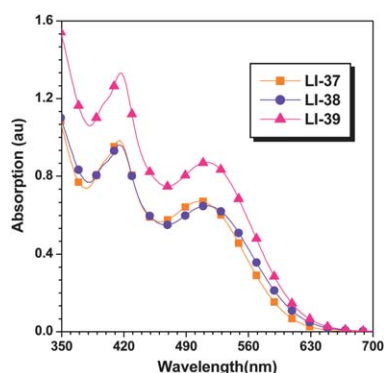


Chart 3



Scheme 1 Synthetic route to sensitizers.

as their extinction coefficients are summarized in Table 1. In the visible region, all of these organic sensitizers show two distinct absorptions around 415 and 510 nm, the absorption band around 415 nm is assigned to a  $\pi$ - $\pi^*$  transition, while the absorption band with  $\lambda_{\text{max}}$  around 510 nm is corresponded to an ICT between the triphenylamine donor part and the acceptor end group. The red-shifted ICT band was obvious due to the strong electron-drawing ability of the auxiliary acceptor in the  $\pi$ -conjugated space, which decreases the band gap and optimizes the energy levels, resulting in a broader responsive wavelength region. In addition, all of the three sensitizers show high molar coefficients ( $>40\,000\text{ M}^{-1}\text{ cm}^{-1}$ ) at the maximum absorption. The absorption peak of **LI-38** (513 nm) and **LI-39** (516 nm) exhibit considerable bathochromic shifts in comparison with that of **LI-37** (504 nm). This result clearly illustrates that the modulation of the optical band-gaps and energy levels of these sensitizers can be partly achieved by altering the electronic nature of triarylamine donors with the addition of the alkyl or alkoxy chains, suggesting that **LI-38** and **LI-39**, the sensitizers bearing stronger donors, possess stronger photoinduced ICT abilities over the  $\pi$ -conjugation backbone, leading to the red-shifted absorption spectra. The absorption spectra of the organic sensitizers anchored onto a transparent nanocrystalline  $\text{TiO}_2$  film (6  $\mu\text{m}$ ) are presented in Fig. 2. After the sensitizers adsorbed on the surface of  $\text{TiO}_2$  films, the absorption peaks located at 520, 525 and 526 nm, respectively. Compared to those observed in the

Fig. 1 UV-vis spectra of sensitizers in  $\text{CH}_2\text{Cl}_2$ .

solution, the little red shift of the absorption bands demonstrated that the intermolecular aggregations can be suppressed in a large degree by the addition of the BPz unit in the  $\pi$ -conjugated spacer, which would avoid the unnecessary energy loss by the molecular interactions. The absorption spectra of the sensitizers became broadened after adsorption on the  $\text{TiO}_2$  surface with an extended absorption onset above 720 nm, which should favor the light harvesting of the solar cells and thus increase the photocurrent response region, leading to the increase of short-circuit photocurrent density ( $J_{\text{sc}}$ ).

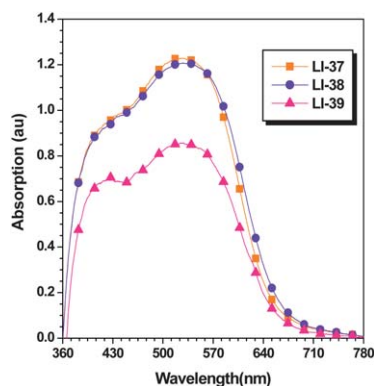
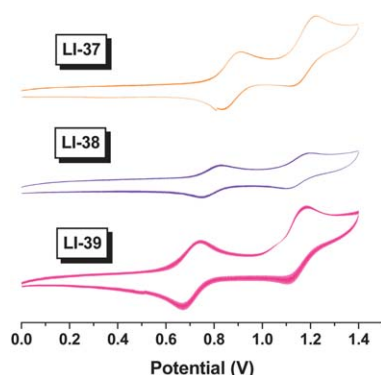
### Electrochemical properties

In order to study the possibilities of electron injection from the excited state sensitizers to the conduction band (CB) of the semiconductor and the sensitizer regenerations, the oxidation potentials of the sensitizers were determined by cyclic voltammograms (Fig. 3). The oxidation potential *vs.* NHE ( $E_{\text{ox}}$ ) corresponded to the highest occupied molecular orbital (HOMO), while the reduction potential *vs.* NHE ( $E_{\text{red}}$ ), which corresponded to the lowest unoccupied molecular orbital (LUMO), could be calculated from  $E_{\text{ox}} - E_{0-0}$ . The electrochemical data of the three sensitizers were summarized in Table 1. Two oxidation waves were observed in the voltammograms. The first quasi-reversible oxidation wave at lower oxidation potentials is attributed to the triphenylamine, whereas the higher oxidation potentials with quasi-reversible behavior, were from the spacer. **LI-39** has the lowest oxidation potential because the oxidized triphenylamine can be stabilized by the two electron-donating methoxy moieties and the thiophene unit nearby, and the higher oxidation potential of **LI-37** is ascribed to the poorest ability of electron-donating among these sensitizers. The lower oxidation potentials means the HOMO raising upon the introduction of stronger donors, which agrees well with the calculation and shows the important contribution of the methyl and methoxy groups to HOMO distributions. The reduction potentials also vary significantly with the variation of the donor, which is also identical to the calculations. As shown in Table 1, the HOMO levels are more positive than the iodine/iodide redox potential value (0.4 V *vs.* NHE), indicating that the oxidized sensitizers formed after electron injection into the conduction band of  $\text{TiO}_2$

**Table 1** Absorbance and electrochemical properties of sensitizers

Sensitizer	$\lambda_{\max}^a$ (nm)	$\epsilon \times 10^4$ (M <sup>-1</sup> cm <sup>-1</sup> )	$\lambda_{\max}^b$ (nm)	$E_{0-0}^c$ (eV)	$E_{\text{ox}}^d$ (V) vs. NHE	$E_{\text{red}}^e$ (V) vs. NHE	Calcd $E_{\text{LUMO}}^f$ (eV)	Calcd $E_{\text{HOMO}}^f$ (eV)
<b>LI-37</b>	415, 504	4.34, 3.04	520	1.98	1.01	-0.97	-2.72	-4.91
<b>LI-38</b>	416, 513	4.28, 2.99	525	2.02	0.92	-1.10	-2.70	-4.80
<b>LI-39</b>	417, 516	4.62, 3.21	526	2.04	0.83	-1.21	-2.66	-4.66

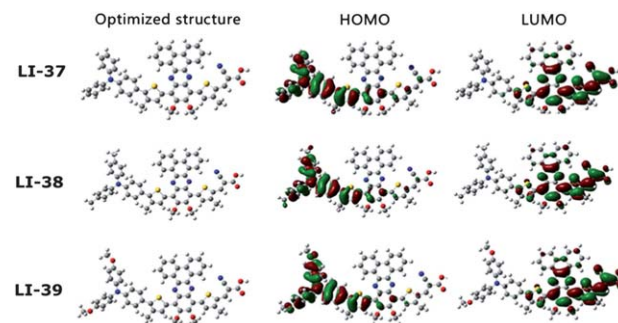
<sup>a</sup> Absorption spectra of sensitizers measured in CH<sub>2</sub>Cl<sub>2</sub> with the concentration of  $3 \times 10^{-5}$  mol L<sup>-1</sup>. <sup>b</sup> Absorption spectra of sensitizers adsorbed on the surface of TiO<sub>2</sub>. <sup>c</sup> The bandgap,  $E_{0-0}$  was derived from the observed optical edge. <sup>d</sup>  $E_{\text{ox}}$  were measured in CH<sub>2</sub>Cl<sub>2</sub> with 0.1 M (*n*-C<sub>4</sub>H<sub>9</sub>)<sub>4</sub>NPF<sub>6</sub> as electrolyte (scanning rate, 100 mV s<sup>-1</sup>; working electrode and counter electrode, Pt wires; reference electrode, Ag/AgCl). The oxidation potential ( $E_{\text{ox}}$ ) referenced to calibrated Ag/AgCl was converted to the NHE reference scale:  $E_{\text{ox}} = E_{\text{ox}}^{\text{on}} + 0.2$  V. <sup>e</sup>  $E_{\text{red}}$  was calculated from  $E_{\text{ox}} - E_{0-0}$ . <sup>f</sup> HOMO and LUMO levels calculated by density functional theory (DFT).

**Fig. 2** UV-vis spectra of the sensitizers on TiO<sub>2</sub> films.**Fig. 3** Cyclic voltammograms of sensitizers in CH<sub>2</sub>Cl<sub>2</sub>.

could thermodynamically accept electrons from I<sub>3</sub><sup>-</sup> ions. The LUMO levels of the sensitizers are sufficiently more negative than the conduction-band-edge energy level ( $E_{\text{cb}}$ ) of the TiO<sub>2</sub> electrode (-0.5 V vs. NHE), which implies that electron injection from the excited sensitizer into the conduction band of TiO<sub>2</sub> is energetically permitted.

### Theoretical approach

The structures of the sensitizers were analyzed using the B3LYP exchange-correlation functional and a 6-31g\* basis set for full geometrical optimization.<sup>12</sup> It is clearly seen from Fig. 4 that the HOMO is distributed along the triphenylamine and first thiophene system, the LUMO is delocalized across the entire A- $\pi$ -A system. The well-overlapped HOMO and LUMO orbitals on the

**Fig. 4** Frontier orbitals of the sensitizers optimized at the B3LYP/6-31+G (D) level.

BPz unit suggest the well inductive or withdrawing electron tendency from triphenylamine donor unit to the cyanoacetic acid unit. After photoexcitation, the electrons in the organic sensitizers loaded on nanocrystalline TiO<sub>2</sub> surface could be successively transferred from the donor to the acceptor unit in spacer, and then transferred to the cyanoacetic acid subunit, and finally into TiO<sub>2</sub>. The calculation of HOMO (Table 1) also reveals the contribution of methyl and methoxy groups to the HOMO distributions in **LI-38** and **LI-39**, which is consistent with their stronger electron-donating nature and the observed bathochromic shifts in absorption spectra. The well-delocalized LUMO over the A- $\pi$ -A units indicates that the additional acceptor of this bulky unit could facilitate the electron transfer from the donor to the acceptor.

### Photovoltaic performance of DSSCs

The photovoltaic characteristics of these sensitizers were obtained with a sandwich cell using the commercial redox electrolyte (DHS-Z23, Heptachroma, China). The action spectra of incident photo-to-current conversion efficiency (IPCE) for DSSCs based on the sensitizers of **LI-37**, **LI-38** and **LI-39** are presented in Fig. 5. The IPCE of the sensitizers illustrated that the visible light can be converted to photocurrent efficiently in the range of 400–700 nm, which was in good accordance with their absorption spectra on the TiO<sub>2</sub> film. The IPCE exceeds 50% in the spectral range 400–570 nm for **LI-39** and **LI-38**, and the maximum value of **LI-39** reaches 65% at 525 nm. From the IPCE curves, we can infer that **LI-38** and **LI-39**, bearing stronger electron donors, have shown higher IPCE values than **LI-37**. Such broader spectral responses of **LI-38** and **LI-39** are consistent with the trend of the absorption spectra, implying their

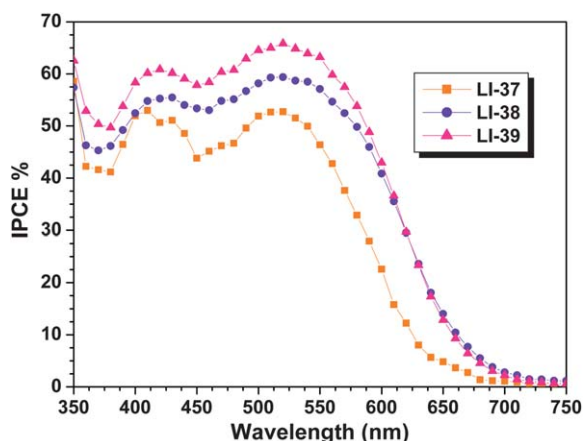


Fig. 5 Spectra of monochromatic incident photon-to-current conversion efficiency (IPCE) for DSSCs based on these sensitizers.

better light harvesting ability for long-wavelength visible light, which would be attributed to the strong electron-withdrawing properties of the BPz unit as well as the good electron-donating abilities of the methyl or methoxyl-substituted triphenylamine unit. Fig. 6 shows the current–voltage characteristics of DSSCs fabricated with these sensitizers under standard global AM 1.5 solar light condition. The detailed parameters of short-circuit current density ( $J_{sc}$ ), open-circuit voltage ( $V_{oc}$ ), fill factor ( $ff$ ), and photovoltaic conversion efficiency ( $\eta$ ) are summarized in Table 2. Each photovoltaic parameter of the devices without CDCA was obtained from several solar cells, which proved the excellent repeatability. All of them showed favorable photovoltaic responses and exhibited the relatively high power conversion efficiencies. The DSSC based on **LI-39** showed the best photovoltaic performance:  $J_{sc}$  of  $14.40 \text{ mA cm}^{-2}$ ,  $V_{oc}$  of  $0.74 \text{ V}$ , and  $ff$  of  $0.67$ , corresponding to the  $\eta$  value of  $7.18\%$ . With relatively lower  $J_{sc}$ , solar cells based on **LI-37** and **LI-38** show relatively inferior efficiencies of  $5.23\%$  and  $6.41\%$ . The three sensitizers have similar chemical structures, but their photovoltaic performances had some differences. The ability of electron-donation could be modified by the methyl or methoxyl-substituted triphenylamine unit. In sensitizers with the D–A'– $\pi$ –A structure, the transport of electron from donor to acceptor could be facilitated by the introduction of strong donor, and as a result, the higher values of  $J_{sc}$  could be obtained.<sup>6</sup> On the other hand, the HOMO and LUMO energy levels were also affected by the

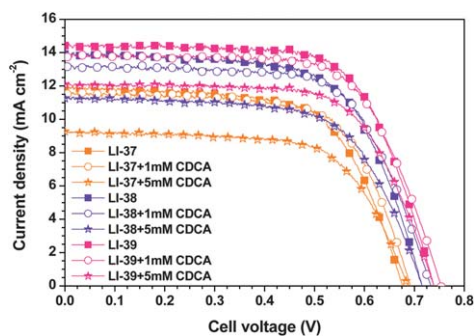


Fig. 6 Current density–voltage characteristics obtained with a nanocrystalline  $\text{TiO}_2$  film supported on FTO conducting glass and derivatized with monolayer of sensitizers.

different donors, in Table 2, the  $J_{sc}$  was consistent with the LUMO energy level of these sensitizers. The reduction potential ( $E_{red}$ ) of the three sensitizers were in the following order: **LI-39** ( $-1.21 \text{ V}$ ) < **LI-38** ( $-1.10 \text{ V}$ ) < **LI-37** ( $-0.97 \text{ V}$ ). **LI-39** shows the most negative reduction potential ( $E_{red}$ ), that is to say, in the process of the electron injection from excited-state sensitizers to the conductive band of  $\text{TiO}_2$ , **LI-39** is the most effective, thus, the cell based on **LI-39** obtains the highest  $J_{sc}$  value. As for the value of  $V_{oc}$ , for the existence of the bulky conjugated unit in the orthogonal directions as well as the long alkyl chains and alkoxy chains in the  $\pi$ -conjugated bridge, the dye aggregates and the charge recombination could be suppressed to a large degree, and the three sensitizers all give the relatively higher  $V_{oc}$  values, in the range of  $0.67$ – $0.74 \text{ V}$ . The charge recombination of cells could be suppressed by the substituent in donor side,<sup>13</sup> for this reason, **LI-37**, with non-substituted triphenylamine donor, possesses the highest level of charge recombination and displays the lowest  $V_{oc}$  of the three. In order to further probe the behavior of the sensitizers on the surface of  $\text{TiO}_2$ , the function of co-adsorbents was investigated. Chenodeoxycholic acid (CDCA) is the most popular co-adsorbent, which binds strongly to the surface of nanostructured  $\text{TiO}_2$ , being able to displace sensitizer molecules from the semiconductor surface and therefore hindering the formation of sensitizer aggregates.<sup>14</sup> Thus, the performances of the DSSCs in the presence of CDCA with various concentrations were studied. The results were collected in Table 2, and the corresponding  $J$ – $V$  curves are shown in Fig. 6. It was found that  $J_{sc}$  decreased dramatically with the increase of the concentration of CDCA, whereas  $V_{oc}$  remained almost the same. Undoubtedly, the amount of sensitizer adsorbed on the  $\text{TiO}_2$  surface was reduced by the coadsorption of CDCA, resulting in a loss of active light harvesting, indicating that CDCA was not necessary for these sensitizers to improve their performance. The result could be considered as a hint that these sensitizers with the introduction of bulky fused aromatic rings to the  $\pi$ -conjugated spacer, did not aggregate on the  $\text{TiO}_2$  surface.

### Electrochemical impedance spectroscopy

To gain more insight into the DSSCs properties, electrochemical impedance spectroscopy (EIS) was performed to analyze the effects on charge recombination, transport and collection. Fig. 7A shows the Nyquist plots for the DSSCs made with  $\text{TiO}_2$  electrodes dipped with the three sensitizers in the dark under a forward bias of  $-0.70 \text{ V}$  with a frequency range of  $0.1 \text{ Hz}$  to  $100 \text{ kHz}$ . The interfacial charge recombination reaction of electrons with the  $\text{I}_3^-$  ions can be described by a charge transfer resistance ( $R_{ct}$ ), which corresponds to the charge transfer processes at the middle frequency range). The interfacial charge recombination reaction of electrons with the  $\text{I}_3^-$  ions can be described by a charge transfer resistance ( $R_{ct}$ ), which corresponds to the charge transfer processes at the  $\text{TiO}_2/\text{dye}/\text{electrolyte}$  interface (a larger semicircle occurs in the middle frequency range). By fitting curves using Z-view software, the values of  $R_{ct}$  were calculated in the order of **LI-39** ( $178.2 \Omega$ ) > **LI-38** ( $102.1 \Omega$ ) > **LI-37** ( $72.87 \Omega$ ). The higher  $R_{ct}$  indicated more effective suppression of the back reaction of the injected electrons with  $\text{I}_3^-$  in the electrolyte and is reflected in the improvements seen in the photocurrent or photovoltage, yielding substantially enhanced device efficiency. Upon illumination under

**Table 2** DSSCs performance data of sensitizers<sup>a</sup>

Sensitizer	CDCA <sup>b</sup>	$J_{sc}$ (mA cm <sup>-2</sup> )	$V_{oc}$ (V)	$ff$	$\eta$ (%)	$\tau_n$ (ms) <sup>c</sup>
LI-37 <sup>d</sup>	None	11.79 ± 0.15	0.680 ± 0.010	0.650 ± 0.005	5.30 ± 0.07	9.8
	1 mM	11.50	0.69	0.67	5.38	
	5 mM	9.26	0.68	0.66	4.22	
LI-38 <sup>d</sup>	None	13.56 ± 0.34	0.725 ± 0.005	0.658 ± 0.005	6.51 ± 0.11	13.6
	1 mM	13.20	0.73	0.66	6.41	
	5 mM	11.25	0.71	0.65	5.27	
LI-39 <sup>d</sup>	None	14.34 ± 0.06	0.741 ± 0.003	0.676 ± 0.003	7.20 ± 0.02	17.3
	1 mM	13.83	0.75	0.67	7.01	
	5 mM	12.08	0.74	0.67	6.01	

<sup>a</sup> Illumination: 100 mW cm<sup>-2</sup> simulated AM 1.5G solar light. <sup>b</sup> Expose to CDCA solution for 6 h before the sensitizer bath. <sup>c</sup> The lifetime ( $\tau_n$ ) of injected electrons in the films can be drawn by the positions of the low-frequency peak in Fig. 7 through the expression  $\tau_n = 1/(2\pi f)$ , in which  $f$  is the frequency of the superimposed ac voltage. <sup>d</sup> Each result without CDCA was obtained from three DSSCs.

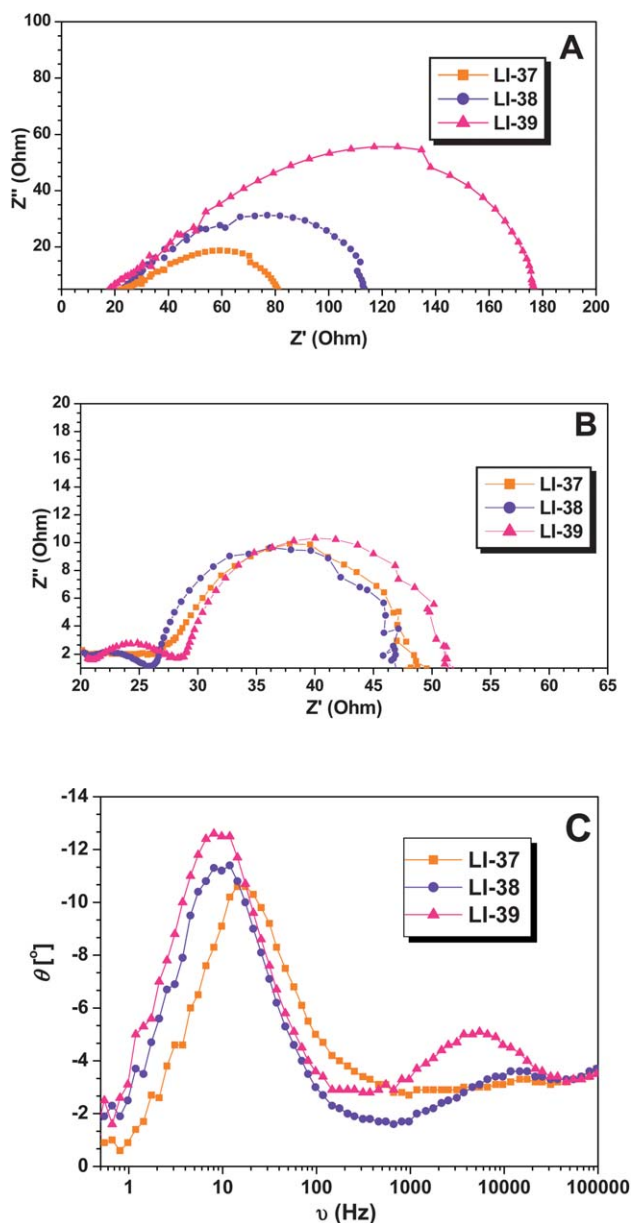


**Fig. 7** Electrochemical impedance spectroscopy (EIS) for DSSCs based on the sensitizers. (A) Nyquist plots in the dark, (B) Nyquist plots under illumination, (C) Bode phase plots under illumination.

open-circuit conditions (100 mW cm<sup>-2</sup>), the radius of the three intermediate-frequency semicircles in the Nyquist plot (Fig. 7B) were similar to each other, indicating that the differences of the electron transport resistance of the three sensitizers were tiny. However, from the characteristic frequency of the middle frequency peak in the Bode phase plot (Fig. 7C), the electron lifetime of sensitizers LI-37 to LI-39 is 9.8, 13.6 and 17.3 ms respectively. The relatively long lifetime indicated that four alkyl chains or alkoxy chains in the spacer of the molecular, blocked the charge recombination effectively. Longer lifetime resulted in better performance in  $J_{sc}$  and  $V_{oc}$ , the results of the electron lifetime are consistent with those parameters in photovoltaic characteristics. Therefore, the larger charge recombination resistance in the dark and long electron lifetime may be the main reason for the higher  $V_{oc}$  value (0.67–0.75 V) of DSSCs based on these sensitizers.

## Conclusion

In summary, we successfully synthesized a series of metal-free organic sensitizers by exploiting 11,12-bis (hexyloxy) dibenzo [*a,c*]phenazine unit as an auxiliary acceptor in the  $\pi$ -conjugated bridge to form the D- $\pi$ -A'- $\pi$ -A system. This planar bulky fused aromatic rings make the three sensitizers exhibit anti-aggregate effect, higher open circuit voltage and good visible light spectrum response. With the proper adjustment of the electron donating abilities, the level of the bathochromic shift could be enhanced, and the photovoltaic performance is consistent entirely. Among them, LI-39 based cell shows the best light to electricity conversion efficiency of 7.18% ( $J_{sc} = 14.40$  mA cm<sup>-2</sup>,  $V_{oc} = 0.74$  V,  $ff = 0.67$ ) without any co-adsorbent. It is believed that these results are indicative for the development of highly efficient metal-free organic sensitizers in the future.

## Acknowledgements

We are grateful to the National Science Foundation of China (no. 21002075), the National Natural Science Foundation of China (no. 61106056) and the National Fundamental Key Research Program (no. 2011CB932702) for financial support.

## Notes and references

- (a) N. Armaroli and V. Balzani, *Angew. Chem., Int. Ed.*, 2007, **46**, 52; (b) A. Listorti, B. O'Regan and J. R. Durrant, *Chem. Mater.*, 2011, **23**,

- 3381; (c) A. Hagfeldt, G. Boschloo, L. Sun, L. Kloo and H. Pettersson, *Chem. Rev.*, 2010, **110**, 6595; (d) B. O'Regan and M. Grätzel, *Nature*, 1991, **353**, 737; (e) Z. Ning and H. Tian, *Chem. Commun.*, 2009, 5483; (f) J. H. Yum, E. Baranoff, S. Wenger, M. K. Nazeeruddin and M. Grätzel, *Energy Environ. Sci.*, 2011, **4**, 842; (g) G. Calogero, G. Di Marco, S. Cazzanti, S. Caramori, R. Argazzi and C. A. Bignozzi, *Energy Environ. Sci.*, 2009, **2**, 1162.
- 2 (a) F. Gao, Y. Wang, D. Shi, J. Zhang, M. Wang, X. Jing, R. Humphry-Baker, P. Wang, S. M. Zakeeruddin and M. Grätzel, *J. Am. Chem. Soc.*, 2008, **130**, 10720; (b) Y. Chiba, A. Islam, Y. Watanabe, R. Komiyama, N. Koide and L. Y. Han, *Jpn. J. Appl. Phys., Part 2*, 2006, **45**, L638.
- 3 (a) A. Mishra, M. K. R. Fischer and P. Bäuerle, *Angew. Chem., Int. Ed.*, 2009, **48**, 2474; (b) Y. Ooyama and Y. Harima, *Eur. J. Org. Chem.*, 2009, 2903; (c) Y. Yen, H. Chou, Y. Chen, C. Hsu and J. T. Lin, *J. Mater. Chem.*, 2012, **22**, 8734.
- 4 (a) W. Li, Y. Wu, X. Li, Y. Xie and W. Zhu, *Energy Environ. Sci.*, 2011, **4**, 1830; (b) Z. Ning, Y. Fu and H. Tian, *Energy Environ. Sci.*, 2010, **3**, 1170; (c) T. Horiuchi, H. Miura, K. Sumioka and S. Uchida, *J. Am. Chem. Soc.*, 2004, **126**, 12218; (d) T. Horiuchi, H. Miura and S. Uchida, *Chem. Commun.*, 2003, 3036; (e) K. Hara, M. Kurashige, S. Ito, A. Shinpo, S. Suga, K. Sayama and H. Arakawa, *Chem. Commun.*, 2003, 252; (f) T. Kitamura, M. Ikeda, K. Shigaki, T. Inoue, N. A. Anderson, X. Ai, T. Lian and S. Yanagida, *Chem. Mater.*, 2004, **16**, 1806; (g) K. Hara, T. Sato, R. Katoh, A. Furube, T. Yoshihara, M. Murai, M. Kurashige, S. Ito, A. Shinpo, S. Suga and H. Arakawa, *Adv. Funct. Mater.*, 2005, **15**, 246.
- 5 (a) Q. Li, L. Lu, C. Zhong, J. Huang, Q. Huang, J. Shi, X. Jin, T. Peng, J. Qin and Z. Li, *Chem.–Eur. J.*, 2009, **15**, 9664; (b) Q. Li, L. Lu, C. Zhong, Q. Huang, J. Shi, X. Jin, T. Peng, J. Qin and Z. Li, *J. Phys. Chem. B*, 2009, **113**, 14588; (c) H. Chou, Y. Chen, H. Huang, T. Lee, J. T. Lin, C. Tsai and K. Chen, *J. Mater. Chem.*, 2012, **22**, 10929; (d) B. Liu, W. Zhu, Q. Zhang, W. Wu, M. Xu, Z. Ning, Y. Xie and H. Tian, *Chem. Commun.*, 2009, 1766; (e) K. Sayama, S. Tsukagoshi, K. Hara, Y. Ohga, A. Shinpo, Y. Abe, S. Suga and H. Arakawa, *J. Phys. Chem. B*, 2002, **106**, 1363; (f) K. Sayama, K. Hara, N. Mori, M. Satsuki, S. Suga, S. Tsukagoshi, Y. Abe, H. Sugihara and H. Arakawa, *Chem. Commun.*, 2000, 1173; (g) Q. H. Yao, L. Shan, F. Y. Li, D. D. Yin and C. H. Huang, *New J. Chem.*, 2003, **27**, 1277; (h) D. Heredia, J. Natera, M. Gervaldó, L. Otero, F. Fungo, C. Y. Lin and K. T. Wong, *Org. Lett.*, 2010, **12**, 12; (i) W. Zeng, Y. Cao, Y. Bai, Y. Wang, Y. Shi, M. Zhang, F. F. Wang, C. Y. Pan and P. Wang, *Chem. Mater.*, 2010, **22**, 1915; (j) J. Shi, Z. Chai, C. Zhong, W. Wu, J. Hua, Y. Dong, J. Qin, Q. Li and Z. Li, *Dyes Pigm.*, 2012, **95**, 244; (k) Q. Li, J. Shi, H. Li, S. Li, C. Zhong, F. Guo, M. Peng, J. Hua, J. Qin and Z. Li, *J. Mater. Chem.*, 2012, **22**, 6689; (l) M. Lu, M. Liang, H. Han, Z. Sun and S. Xue, *J. Phys. Chem. C*, 2011, **115**, 274.
- 6 (a) W. Zhu, Y. Wu, S. Wang, W. Li, X. Li, J. Chen, Z. Wang and H. Tian, *Adv. Funct. Mater.*, 2011, **21**, 756; (b) Y. Cui, Y. Wu, X. Lu, X. Zhang, G. Zhou, F. B. Miapheh, W. Zhu and Z. Wang, *Chem. Mater.*, 2011, **23**, 4394; (c) Y. Wu, X. Zhang, W. Li, Z. Wang, H. Tian and W. Zhu, *Adv. Energy Mater.*, 2012, **2**, 149.
- 7 S. Huang, Y. Hsu, Y. Yen, H. Chou, J. T. Lin, C. Chang, C. Hsu, C. Tsai and D. Yin, *J. Phys. Chem. C*, 2008, **112**, 19739.
- 8 (a) Z. Wang, N. Koumura, Y. Cui, M. Takahashi, H. Sekiguchi, A. Mori, T. Kubo, A. Furube and K. Hara, *Chem. Mater.*, 2008, **20**, 3993; (b) Z. Ning, Q. Zhang, H. Pei, J. Luan, C. Lu, Y. Cui and H. Tian, *J. Phys. Chem. C*, 2009, **113**, 10307.
- 9 S. Li, Z. He, J. Yu, S. Chen, A. Zhong, R. Tang, H. Wu, J. Qin and Z. Li, *J. Mater. Chem.*, 2012, **22**, 12523.
- 10 M. Reggelen, J. Scholz and M. Hamburger, *J. Polym. Sci., Part A: Polym. Chem.*, 2009, **47**, 4830.
- 11 (a) D. Chang, H. Lee, J. Kim, S. Park, S. Park, L. Dai and J. Baek, *Org. Lett.*, 2011, **13**, 3880; (b) K. Pei, Y. Wu, W. Wu, Q. Zhang, B. Chen, H. Tian and W. Zhu, *Chem.–Eur. J.*, 2012, **18**, 8190.
- 12 M. J. Frisch, G. W. Trucks, H. B. Schlegel, G. E. Scuseria, M. A. Robb, J. R. Cheeseman, J. A. Montgomery, Jr, T. Vreven, K. N. Kudin, J. C. Burant, J. M. Millam, S. S. Iyengar, J. Tomasi, V. Barone, B. Mennucci, M. Cossi, G. Scalmani, N. Rega, G. A. Petersson, H. Nakatsuji, M. Hada, M. Ehara, K. Toyota, R. Fukuda, J. Hasegawa, M. Ishida, T. Nakajima, Y. Honda, O. Kitao, H. Nakai, M. Klene, X. Li, J. E. Knox, H. P. Hratchian, J. B. Cross, C. Adamo, J. Jaramillo, R. Gomperts, R. E. Stratmann, O. Yazyev, A. J. Austin, R. Cammi, C. Pomelli, J. W. Ochterski, P. Y. Ayala, K. Morokuma, G. A. Voth, P. Salvador, J. J. Dannenberg, V. G. Zakrzewski, S. Dapprich, A. D. Daniels, M. C. Strain, O. Farkas, D. K. Malick, A. D. Rabuck, K. Raghavachari, J. B. Foresman, J. V. Ortiz, Q. Cui, A. G. Baboul, S. Clifford, J. Cioslowski, B. B. Stefanov, G. Liu, A. Liashenko, P. Piskorz, I. Komaromi, R. L. Martin, D. J. Fox, T. Keith, M. A. Al-Laham, C. Y. Peng, A. Nanayakkara, M. Challacombe, P. M. W. Gill, B. Johnson, W. Chen, M. W. Wong, C. Gonzalez and J. A. Pople, *Gaussian 09, Revision E.1*, Gaussian, Inc., Pittsburgh, PA, 2009.
- 13 D. Hagberg, X. Jiang, E. Gabrielsson, M. Linder, T. Marinado, T. Brinck, A. Hagfeldt and L. Sun, *J. Mater. Chem.*, 2009, **19**, 7232.
- 14 S. Ito, H. Miura, S. Uchida, M. Takata, K. Sumioka, P. Liska, P. Comte, P. Péchy and M. Grätzel, *Chem. Commun.*, 2008, 5194.